



Cite this: *Ind. Chem. Mater.*, 2024, 2, 173

## Recent progress of antipoisoning catalytic materials for high temperature proton exchange membrane fuel cells doped with phosphoric acid

Dongping Xue and Jia-Nan Zhang \*

High-temperature proton exchange membrane fuel cells (HT-PEMFCs) have the unique advantages of fast electrode reaction kinetics, high CO tolerance, and simple water and thermal management at their operating temperature (120–300 °C), which can effectively solve the hydrogen source problem and help achieve the dual-carbon goal. The catalysts in HT-PEMFCs are mainly Pt-based catalysts, which have good catalytic activity in the oxygen reduction reaction (ORR) and hydrogen oxidation reaction (HOR). However, in HT-PEMFCs, the high load of platinum-based catalysts to alleviate the limitation of strong adsorption of phosphoric acid (PA) on the platinum surface on activity expression leads to high cost, insufficient activity, decreased activity under long-term operation and carrier corrosion. The present review mainly summarizes the latest research progress of HT-PEMFCs catalysts, systematically analyzes the application of precious metal and non-precious metal catalysts in HT-PEMFCs, and unveils the structure–activity relationship and anti-PA poisoning mechanism. The current challenges and opportunities faced by HT-PEMFCs are discussed, as well as possible future solutions. It is believed that this review can provide some inspiration for the future development of high-performance HT-PEMFC catalysts.

**Keywords:** High-temperature proton exchange membrane fuel cells; Cathodic oxygen reduction; Anti-phosphoric acid poisonous; Pt group metal catalysts; Non-precious metal catalysts.

Received 14th September 2023,  
Accepted 19th October 2023

DOI: 10.1039/d3im00101f

rsc.li/icm

### 1 Introduction

A fuel cell is an electrochemical energy device that converts chemical energy directly into electric energy.<sup>1</sup> It has many advantages, such as high power density, high energy

College of Materials Science and Engineering, Zhengzhou University, Zhengzhou 450001, P. R. China. E-mail: zjn@zzu.edu.cn



**Dongping Xue**

*Dongping Xue is currently a Ph.D. candidate at the College of Materials Science and Engineering, Zhengzhou University, majoring in Materials Science and Engineering. She has been working in Professor Jia-Nan Zhang's group since 2020. Her work focuses on the electrochemical applications of carbon nanomaterials as catalysts for oxygen reduction reactions in fuel cells and zinc-air batteries.*



**Jia-Nan Zhang**

*Jia-Nan Zhang received her BSc. (2005) and Ph.D. (2010) degrees from the State Key Laboratory of Inorganic Synthesis and Preparative Chemistry at Jilin University, supervised by Profs. Ruren Xu and Jihong Yu. During this, she was at Oak Ridge National Laboratory, U. S.A., as a visitor researcher. She was an academic visitor at the National Institute of Advanced Industrial Science and Technology (AIST) of Japan in 2018–2019. Currently, she is a full Professor at the College of Materials Science and Engineering, Zhengzhou University. Her research interest focuses on carbon-based nano-functional materials for energy conversion and storage.*



conversion efficiency, and low environmental pollution, and can be widely used in portable power supplies and electric vehicles.<sup>2–4</sup> Therefore, the development of fuel cell technology is of great social significance to solve energy and environmental problems. The high-temperature proton exchange membrane fuel cell (HT-PEMFC), with an operating temperature of 120–300 °C, uses a phosphoric acid (PA) doped polymer material as the high-temperature membrane, overcoming the problems existing in the traditional low-temperature proton exchange membrane fuel cell (LT-PEMFCs  $\approx$  70–95 °C)<sup>5–7</sup> as follows: 1) accelerating the reaction kinetics with the assistance of thermo-electric coupling; 2) simplifying the thermal and water management because the high-temperature system has no liquid and thus providing high system utilization; 3) increasing the tolerance of the electrocatalyst to poisonous gases, which means that the reformed gas can be directly used as fuel for HT-PEMFCs. However, there are still some challenges associated with HT-PEMFCs, such as possible corrosion, mechanical failure of the bipolar plates, and degradation of the catalyst/catalyst support, catalyst layer and proton exchange membrane (PEM) at high-temperature,<sup>8</sup> as well as insufficient heating strategies to achieve and maintain the high operating temperature for long-term functioning of HT-PEMFC stacks.<sup>9</sup> More importantly, in PA-doped PEM, PA molecules exist in the network structure of polymer chains in two forms: bound and free.<sup>10,11</sup> The bound form of PA is anchored around the polymer chain by strong hydrogen bonding, while the free form of PA has weak interactions with polymer molecules, mainly forming a hydrogen bonding network between PA molecules, which is the main mode of proton transfer.<sup>12–14</sup> Therefore, higher free PA doping can achieve higher proton

conductivity. However, PA is distributed and migrated within the electrolyte membrane electrode assembly (MEA) by various factors. As shown in Fig. 1, during the operation of the cell, PA in the membrane is driven by current, and the  $\text{H}_2\text{PO}_4^-$  hydrolyzed by PA migrates from the membrane to the anode and reacts with hydrogen ions on the anode side to form PA, thereby increasing the anode PA content.<sup>15,16</sup> Subsequently, due to the concentration gradient difference, PA diffuses to the cathode and combines with the cathode product water to form  $\text{H}_2\text{PO}_4^-$ . This cycle promotes the redistribution of PA in the catalytic layer, resulting in the phenomenon of “acid flooding” in the catalytic layer.<sup>17,18</sup> In addition, a large number of PA and PA dissociated ions occupy the active sites of the platinum catalyst. The material transport resistance in the catalytic layer increases and the reaction kinetics is slow, which seriously hinders the large-scale commercialization of HT-PEMFCs.<sup>19</sup> Therefore, it is necessary and economically desirable to develop electrocatalysts with high efficiency, durability, and high PA tolerance in HT-PEMFCs.

In hydrogen fuel cells, the hydrogen oxidation and oxygen reduction processes on the electrode are mainly controlled by the catalyst. Catalysts can significantly reduce the activation energy of a chemical reaction and change the rate of the chemical reaction.<sup>20</sup> The catalyst is the main factor affecting the activation and polarization of hydrogen fuel cells. It is regarded as the key material of hydrogen fuel cells and determines the performance and use economy of hydrogen fuel cell vehicles.<sup>21</sup> In the reaction process of hydrogen fuel cells, the anode HOR reaction is a fast kinetic process, while the cathode ORR reaction is more complex, involving the multi-step gain and loss of electrons and the transfer of



Fig. 1 Distribution and migration of phosphoric acid in membrane electrode.



coupled protons, which is a slow kinetic process. Compared with HOR, ORR is 6 orders of magnitude slower, so ORR is considered to be one of the major performance limiting factors in HT-PEMFCs as well as LT-PEMFCs. Compared to LT-PEMFCs, a larger amount of precious metal is needed to overcome the negative effect of PA existence in HT-PEMFCs. This is why developing ORR catalysts has been the major effort in PEMFC studies during the last two decades.<sup>22–24</sup> Overall, developing catalysts with low cost, high performance, and excellent durability is the main goal of the commercial application of HT-PEMFC. According to the Sabatier principle, there is a typical volcanic curve relationship between the catalytic activity of ORR and different transition metals. Platinum (Pt) is located at the top of the volcano and has the best ORR activity (Fig. 2), which is also the reason why Pt/C catalysts can be commercialized at present.<sup>25,26</sup> However, Pt resources are scarce and expensive, resulting in the cost of the catalyst accounting for a large part of the overall cost of the fuel cell system. In addition, the Pt/C catalyst under fuel cell conditions has Ostwald ripening, carbon carrier corrosion and other problems, which are more severe in HT-PEMFCs and seriously affect the service life.<sup>27</sup> Therefore, how to reduce the Pt load while solving the problems of slow cathode ORR kinetics and PA poisoning plays a vital role in reducing the catalyst cost of HT-PEMFCs.<sup>25,28</sup>

In order to make up for the shortcomings of Pt/C catalysts and achieve the above goals, novel and effective catalysts have been gradually developed in the research of catalysts for HT-PEMFCs. Adding another element to Pt nanoparticles to adjust the electronic structure of Pt nanoparticles, alloying Pt with other metals, or constructing core-shell structures are optimization strategies to overcome the lack of activity and stability.<sup>25,26,29</sup> On the other hand, researchers are committed to finding cheap metal catalysts that can replace Pt group metals. Among these, single atom catalysts (SACs) have attracted widespread attention due to their atomic dispersion, high atomic utilization, and comparable activity with traditional metal particle catalysts.<sup>30</sup> Transition metal based SACs have better ORR catalytic activity and lower cost, and are a potential substitute for Pt-based ORR catalysts in



Fig. 2 Trends in oxygen reduction activity (defined in the text) plotted as a function of the oxygen binding energy. Reprinted with permission from ref. 26. Copyright 2004, American Chemical Society.

fuel cells.<sup>31</sup> However, the stability of SACs and the dissolution of metal sites still need to be addressed urgently. In addition, previous studies have shown that, based on the concept of the third layer of zeolite effect, the design and synthesis of some organic molecules containing cyanide ions, melamine and sulfhydryl groups as barrier materials can effectively prevent the poison effect of phosphate anions in HT-PEMFCs.<sup>32,33</sup> However, in high-temperature operating systems, chemically modified organic molecules may detach from the surface of metal nanoparticles. Therefore, from a practical application perspective, it is difficult to maintain the zeolite effect during long-term operation of HT-PEMFCs.

Herein, we present a critical review on the research and development of the anti-phosphate poisoning effect of catalysts for ORR, with a focus on the mechanistic understanding of anti-phosphate poisoning from both the experimental and theoretical perspectives, elucidation of the structure–property relationship, and strategic improvement of the catalytic activity/selectivity/durability for applications in practical HT-PEMFCs. Fig. 3 displays the main types of catalysts used in HT-PEMFCs.

## 2 Cathode catalysts for HT-PEMFCs

For an effective ORR catalyst, high activity and durability can be achieved by optimizing structural engineering with nanostructures, alloying, intercalating, and confining of active elements or compounds in the desired materials, which should have favorable composition and defects as the catalyst support. The ORR catalysts (Pt based catalysts and non-precious metal-based catalysts) applied to HT-PEMFC will be discussed in detail in the following sections.

### 2.1 Precious metal catalysts

The four electron ORR pathway can be carried out through several mechanisms (Fig. 4). The direct four electron mechanism can essentially be dissociative or associative, depending on the oxygen dissociation barrier on the catalyst surface. The indirect four electron mechanism first involves



Fig. 3 Schematic illustration of the direct four-electron ORR pathway. The red and blue arrows represent the associative and dissociative pathways, respectively. The purple arrows represent the reactions that take place in both pathways.



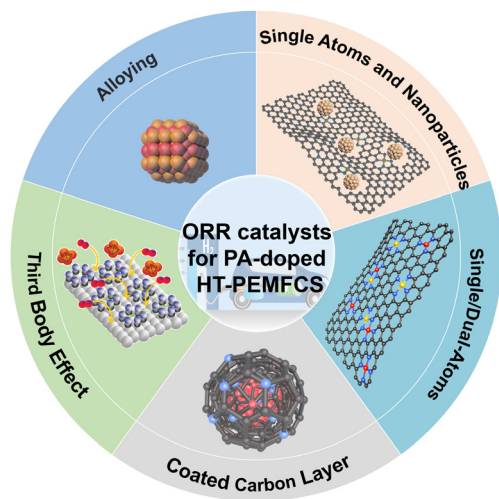


Fig. 4 The main types of catalysts used in HT-PEMFCs.

the two electron pathway of hydrogen peroxide, which is further reduced to  $\text{H}_2\text{O}$ .<sup>34</sup> Nørskov *et al.* established a volcanic map related to theoretical ORR activity and  $\Delta E_{\text{O}}$ , as shown in Fig. 2.<sup>26</sup> For metals that bind too strongly to oxygen, their activity is limited by the transfer of proton electrons to  $\text{O}^*$  or  $\text{OH}^*$ . On the other hand, for metals that are too weakly bound to oxygen, their activity is limited by proton electron transfer to  $\text{O}_2^*$  (association mechanism) or  $\text{O}-\text{O}$  bond splitting in  $\text{O}_2$  (dissociation mechanism). Pt is located near the top of the volcanic curve, with the best ORR catalytic activity, but there is still some room for improvement. Reducing the binding energy between the intermediate and Pt by approximately 0.2 eV can further enhance the activity. Furthermore, Nørskov *et al.* proposed the d-band center theory based on the relationship between the d-band centers of metals and the binding energy of adsorbents on metals.<sup>35</sup> The level of the d-band center determines the degree to which the anti-bond band is filled by electrons and thus determines the stability and strength of the adsorption bond. The downward shift of the d-band center of Pt relative to the Fermi level can weaken the binding between ORR intermediates and metal surfaces, thereby improving the catalytic activity of ORR.<sup>36</sup> In summary, finding a method to reduce the d-band center of Pt will further enhance the catalytic activity of ORR, reduce ORR overpotential, and lead to weaker adsorption of phosphorus anions and hydroxide anions.

The adsorption of phosphate anions on Pt presents an additional complication in the sense that PA has polyprotic properties with three proton dissociation constants. Thus, the species and mode of phosphate anion adsorption on Pt is highly dependent not only on the pH, but also on the potential, the morphology and crystal orientation of the Pt, and so on.<sup>37,38</sup> Tanaka *et al.* proposed that phosphate anions adsorb three oxygen atoms on a Pt(111) surface in a 3-fold site, but only one or two oxygen atoms on Pt(100) and Pt(110) surfaces.<sup>39</sup> This is consistent with the most pronounced

poisoning effect by phosphate anions observed on Pt(111) surfaces, as compared to those on Pt(100) and Pt(110) surfaces.<sup>40</sup> Based on the above results, it is reasonable to deduce that the adsorption of phosphate anions on Pt could be suppressed in part by altering the crystalline facets on the surface. Chen *et al.* found that Pt(111)Sn has the tendency to mitigate anion adsorption on Pt in acid media by freeing more active sites *via* an apparent electronic or ligand effect.<sup>40</sup> These findings also demonstrate that introducing the second type of element may help release Pt sites from phosphate anions, thereby improving ORR performance. Mukerjee *et al.* used *in situ* X-ray absorption  $\Delta\mu$  technology to analyze the adsorption coverage and phosphate anion adsorption sites on the surface of Pt and PtNi alloys to understand the role and mechanism of phosphate anion poisoning in ORR.<sup>41</sup> It has been found that 1/4 of the surface sites are occupied by Ni on PtNi, which lowers the number of “pure” 3-fold Pt sites on the surface. Rotating disc electrode (RDE) experiments show a smaller shift of the half-wave potential in the ORR polarization curves for PtNi/C than for Pt/C upon adding  $\text{H}_3\text{PO}_4$  into 0.1 M  $\text{HClO}_4$  solution (Fig. 5a and b). On the surface of the Pt–Ni catalyst, due to the low sensitivity of the Pt–Ni catalyst to  $\text{H}_2\text{PO}_4^-$  ion poisoning,  $\text{OH}^*$  blocks ORR, the phosphate lateral interactions keep  $\text{OH}^*$  off the surface and more sites are available for the ORR (Fig. 5c and d). Intermetals with the same composition as alloys but an ordered structure exhibit high activity and robust stability, but their active expression is still limited in the presence of PA. Therefore, additional adjustment is essential for Pt-based catalysts to maintain good activity and robust stability in the PA environment. Strain engineering, such as compressive or tensile strain generated by lattice mismatch with different structures or components, can accelerate the reaction kinetics by regulating the d-band center of metal-based materials and altering the binding energies toward adsorbates.<sup>42,43</sup> Wang *et al.* used a small amount of Cu as a doping agent to enhance HT-PEMFC for the first time and improved the phosphate resistance of PtFe ordered intermetallic alloys through a doping modulation strain strategy.<sup>44</sup> This Cu doping facilitates the formation of compressive strain in PtFe crystals, altering the electronic structure of the electrocatalysts and then weakening the adsorption energy between PA and the Pt surfaces, and consequently improving the HT-PEMFC performance (Fig. 6a–c). As a result, the Cu–PtFe/NC electrocatalysts display outstanding performance ( $793.5 \text{ mW cm}^{-2}$ ) with a low Pt loading of  $0.5 \text{ mg}_{\text{Pt}} \text{ cm}^{-2}$  in HT-PEMFC and deliver a current density of  $0.2 \text{ A cm}^{-2}$  at 0.7 V for at least 100 h (Fig. 6d and e). This study provides a novel and general method for regulating the phosphate adsorption behavior on the Pt surface in HT-PEMFCs to fine-design efficient and robust electrocatalysts through lattice strain.

Commercial Pt/C catalysts consist of Pt nanoparticles and carbon supports. Carbon materials usually have a large specific surface area, good conductivity, and abundant loading sites which can load a large amount of metals





Fig. 5 Disk current density (based on the geometric area of the electrode) obtained during ORR on (a) Pt/C and (b) PtNi/C; (c) experimental  $\Delta\mu$  spectra for Pt/C and PtNi/C taken at 0.54 V in 0.1 M HClO<sub>4</sub> with addition of various amounts of H<sub>3</sub>PO<sub>4</sub> and concentrated H<sub>3</sub>PO<sub>4</sub>, (d)  $\Delta\mu$  XANES spectra obtained with Pt/C and PtNi at the Pt L<sub>3</sub> edge in 0.1 M HClO<sub>4</sub> and 100 mM H<sub>3</sub>PO<sub>4</sub> at the different potentials indicated. Reprinted with permission from ref. 41. Copyright 2013, American Chemical Society.



Fig. 6 (a) The charge density difference of the Cu–PtFe crystals; (b) geometric structures and PA adsorption strength of H<sub>2</sub>PO<sub>4</sub><sup>−</sup> adsorption on Cu–PtFe and PtFe; (c) the  $E_{1/2}$  of all catalysts in the electrolyte of HClO<sub>4</sub> and HClO<sub>4</sub> and PA; (d) H<sub>2</sub>–O<sub>2</sub> fuel cell polarization curves and corresponding power densities; (e) durability test results; (f) H<sub>2</sub>–air fuel cell. Reprinted with permission from ref. 44. Copyright 2021, Wiley-VCH.



without agglomeration. However, the harsh working conditions, high potential, continuous oxygen introduction, and strong acid environment of fuel cells inevitably result in carbon corrosion during long-term operation. Therefore, under harsh fuel cell conditions, using more stable and durable carriers will better improve the catalytic activity of Pt based catalysts. In addition, special modifications to carbon supports will affect the application prospects of Pt nanoparticles (NPs) and also enhance their stability. Silica ( $\text{SiO}_2$ ), although it is inactive for ORR, is well known for strong H-bonding capability to acids, which is beneficial to prevent acid leaching and improve stability.<sup>45,46</sup> Based on this, Huang *et al.* prepared  $\text{CNT@SiO}_2\text{-Pt}$  cathode catalysts by modifying carbon nanotubes with  $\text{SiO}_2$  and further loading Pt NPs.<sup>47</sup> The strong adsorption of the phosphate ions on the  $\text{SiO}_2$  of  $\text{CNT@SiO}_2\text{-Pt}$  relieved the phosphate poisoning on Pt, promoted the uniform distribution of PA in the catalytic layer and provided proton chains to assist the

ORR in the HT-PEMFCs (Fig. 7a and b).  $\text{CNT@SiO}_2\text{-Pt}$  cathode catalysts exhibited high activity for ORR and superior power densities of  $765 \text{ mW cm}^{-2}$  ( $\text{H}_2/\text{O}_2$ ) and  $486 \text{ mW cm}^{-2}$  ( $\text{H}_2/\text{air}$ ) without back pressure at  $160 \text{ }^\circ\text{C}$  for HT-PEMFCs (Fig. 7c and d). More importantly, due to the limiting effect of  $\text{SiO}_2$ , the aggregation of Pt NPs is prevented, and they operate stably at a current density of  $200 \text{ mA cm}^{-2}$  (Fig. 7e). In order to further explore the role of  $\text{SiO}_2$ , the influence of phosphate ions on ORR activity was evaluated in  $0.1 \text{ M HClO}_4$  electrolyte with the addition of  $0.1 \text{ M H}_3\text{PO}_4$ . The commercial Pt/C showed a serious poisoning effect, and the  $E_{1/2}$  negatively shifted by  $60 \text{ mV}$  after the addition of  $0.1 \text{ M H}_3\text{PO}_4$ . In the case of  $\text{CNT@SiO}_2\text{-Pt}$ , the results revealed that the  $E_{1/2}$  only shifted negatively by  $31 \text{ mV}$  with the addition of  $0.1 \text{ M PA}$ , indicating that the resistance to phosphate poisoning was enhanced due to the presence of  $\text{SiO}_2$  (Fig. 7f-h). Jung *et al.* reasonably designed Pt-based NPs wrapped in ultra-thin carbon shells as an anti-poisoning catalyst for



**Fig. 7** (a) Single cell and  $\text{CNT@SiO}_2\text{-Pt}$  in the catalytic layer of HT-PEMFCs; (b) HR-TEM image of  $\text{CNT@SiO}_2\text{-Pt}$  (inset: HRTEM image of  $\text{CNT@SiO}_2\text{-Pt}$ ); (c and d) polarization and power density curves; (e) potential response of a 100 h HT-PEMFCs life test; (f) ORR polarization curves of  $\text{CNT@SiO}_2\text{-Pt}$ ; cyclic voltammograms of (g) JM-Pt/C and (h)  $\text{CNT@SiO}_2\text{-Pt}$  in  $\text{N}_2$ -saturated electrolyte. Reprinted with permission from ref. 47. Copyright 2021, Springer Nature.



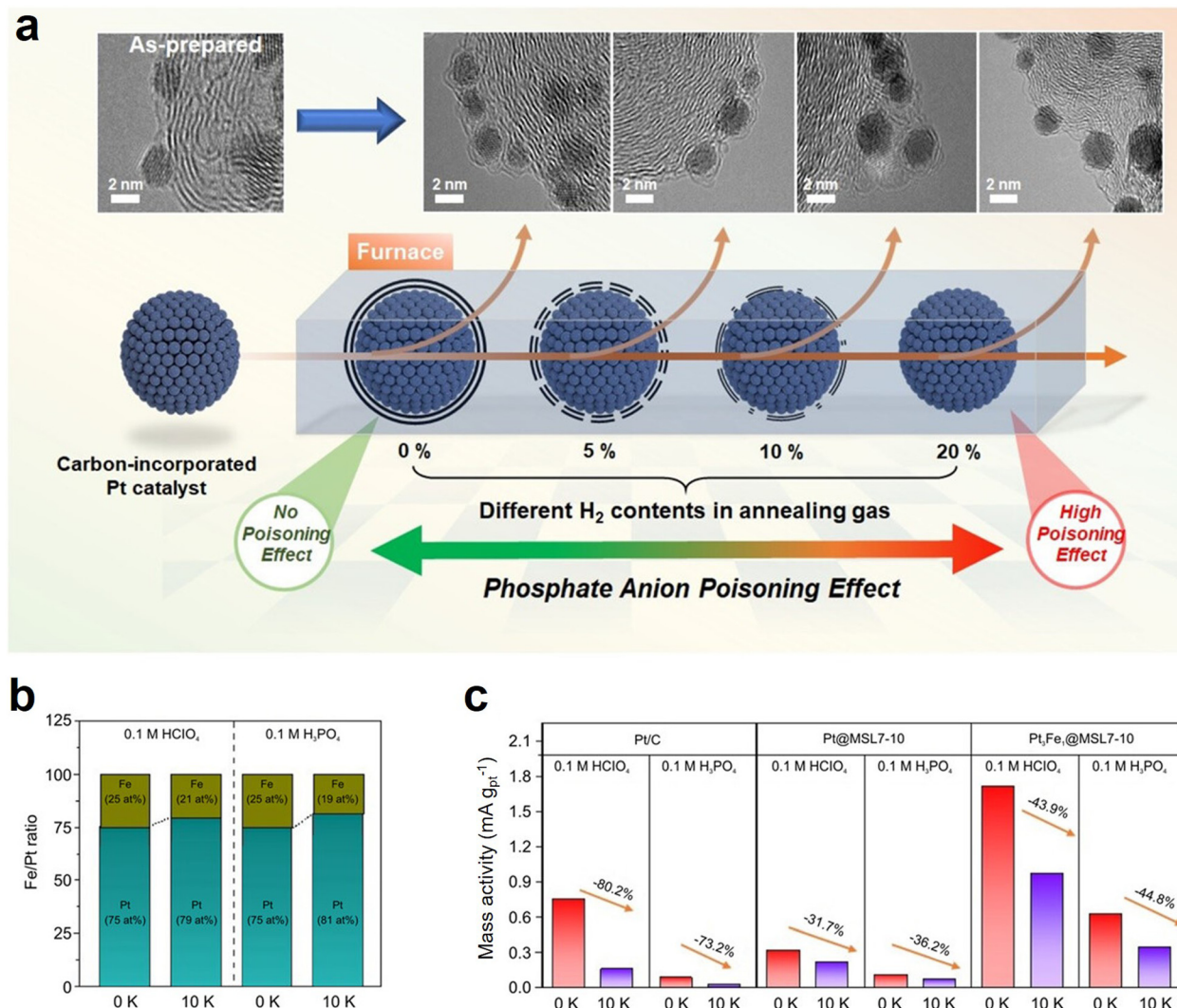


**Fig. 8** (a) Schematic diagram showing the strategy to control the carbon shell structure of Pt-based nanoparticles for realizing the molecular sieve layer effect; (b) Pt/Fe ratios of Pt<sub>3</sub>Fe<sub>1</sub>@MSL7-10 after ADTs; (c) changes in the mass activity of catalysts before and after ADTs. Reprinted with permission from ref. 48. Copyright 2023, John Wiley & Sons.

molecular sieve layers (Fig. 8a).<sup>48</sup> The pore structure of the carbon shells is systematically regulated at the atomic level by high-temperature gas treatment, allowing O<sub>2</sub> molecules to selectively react on the active sites of the metal NPs through the molecular sieves. The ORR activity of Pt and Pt<sub>3</sub>Fe<sub>1</sub> alloy NPs encapsulated in the carbon molecular sieve layer with controllable structure was significantly improved in PA solution (Fig. 8b and c).

More importantly, the carbon shell serves as a protective layer which can effectively prevent the dissolution of metals in the catalyst during long-term operation. It is believed that the carbon shell packaging strategy will provide insights into the design of Pt-based catalysts for high-performance HT-PEMFCs. Phosphide-based compounds show better stability in acidic electrolytes and possess abundant valence electrons compared to transition metal compounds. The combination of Pt with heteroatoms such as P can thus offer a promising approach towards improving the stability and activity of

electrocatalysts.<sup>49–51</sup> For example, Wang *et al.* synthesized controllable sized monodispersed Pt<sub>2</sub> NPs on nitrogen and phosphorus doped carbon (NPC) using a combination of the template and pyrolysis methods and verified their self-conversion process as core-shell Pt/Pt<sub>2</sub> with a thin Pt surface (~1 nm) as an effective ORR catalyst.<sup>52</sup> However, the application of phosphides in HT-PEMFCs is extremely rare. Recently, Yu *et al.* prepared a Pt-based phosphide catalyst using trioctylphosphine (TOP) as a phosphorus source in the presence of Ketjen black (KB) carbon and applied the PtP<sub>2</sub>-based catalyst to the HT-PEMFC cathode for the first time (Fig. 9a).<sup>53</sup> The prepared catalyst exhibits excellent activity and stability under harsh H<sub>3</sub>PO<sub>4</sub> conditions (Fig. 9b and c). In addition, the catalyst structure of phosphorylation also reduces the oxidation of carbon carriers, ultimately helping to maintain the activity of PtP<sub>2</sub>/C-based catalysts. Density functional theory (DFT) calculations have found that this is due to the self-oligomerization effect of surface-bound





**Fig. 9** (a) TEM image of Pt<sub>2</sub>/C-800 electrocatalysts, the inserted bar graph shows the Pt<sub>2</sub> particle size distribution along with the average Pt<sub>2</sub> particle size. (a1) HR-TEM image. (a2) FFT patterns of the area enclosed in the red square in (a1). (a5) HAADF images and the corresponding EDX images of (a1). (a3 and a4) Inverse FFT images of the area enclosed in the red square in (a1), where (a3) shows the distribution of 220 planes while (a4) shows the presence of 200 planes. (b) Mass and specific activity profiles; (c) long-term durability tests of Pt<sub>2</sub>/C-800; (d) free energy diagram for the ORR on four different active site models constructed from the (111) surfaces. Reprinted with permission from ref. 53. Copyright 2023, Royal Society of Chemistry.

phosphorus oxide clusters acting as a phosphate reservoir, thus leaving Pt sites effectively untouched (Fig. 9d). Therefore, to improve the market penetration of HT-PEMFCs, developing a cathode catalyst that can maintain stability in H<sub>3</sub>PO<sub>4</sub> electrolyte and sufficient activity in ORR is one of the key issues to be addressed in the future.

Recently, another strategy to inhibit the adsorption of phosphate anions has been proposed which involves pre-adsorption of CN<sup>-</sup> and other molecules on Pt surfaces, which reduces the availability of triple sites on the Pt surface, thereby inhibiting the adsorption of phosphate anions. This is called the “third-body effect”.<sup>54</sup> Marković *et al.* used the molecular patterning of Pt(111) to develop new concepts for designing ORR catalysts in environments containing strongly adsorbing phosphoric and sulfuric acid anions (Fig. 10a and b).<sup>55</sup> The results confirm that the CN<sub>ad</sub> molecules can block the sites for adsorption of covalently bonded spectator sulfuric/phosphoric anions but still provide a sufficient number of free Pt sites first to chemisorb the O<sub>2</sub> molecule and then to break the O–O bond. Therefore, it is concluded that the adsorption of sulfuric acid and phosphate anions on Pt(111)–CN<sub>ad</sub> is almost completely inhibited by the so-called third body effect. Although the present paper is centered on the Pt(111) surface modified by CN<sub>ad</sub>, fundamental and practical applications go well beyond this system, and should be extremely helpful in the quest to find new directions in designing electrochemical interfaces that can bind selectively reactive and spectator molecules. According to reports, in addition to serving as a third party, electron donating pre-adsorbents can also modify the

electronic structure of Pt in Pt alloys, thereby improving the catalytic activity.<sup>32,33</sup> Among them, oleamine (OA) modified catalyst with a surface coverage of up to 30% of N atom can



**Fig. 10** (a) On Pt(111) covered by phosphoric/sulfuric acid anions, O<sub>2</sub> can access the surface's atoms only through a small number of holes in the adsorbate anion adlayer; (b) the number of holes required for O<sub>2</sub> adsorption is significantly increased on the Pt(111)–CN<sub>ad</sub> surface because adsorption of phosphoric/sulfuric acid anions is suppressed by the CN adlayer so that the total CN<sub>ad</sub>/OH<sub>ad</sub> coverage is lower than the coverage by sulfuric or phosphoric acid anions. Reprinted with permission from ref. 55 Copyright 2010, Springer Nature. (c and d) Schematic presentation of tailoring the d-band structure by surface-capping organic molecules. Reprinted with permission from ref. 56. Copyright 2013, American Chemical Society.



supply electrons to the metal active center by taking advantage of the characteristic that the amine functional group can easily bind to Pt. Chung *et al.* reported that, when commercial Pt/C catalysts were modified, the electronic structure of the Pt NPs was altered, *i.e.*, the d-band center was downshifted, to provide significantly enhanced ORR activity (Fig. 10c and d).<sup>56</sup> In addition, when H<sub>3</sub>PO<sub>4</sub> was added to the electrolyte solution, the OA-adsorbed Pt/C showed enhanced ORR activity retention (up to 71%) compared to the untreated Pt/C (47%) which can be ascribed to the third-body effect of the adsorbed OA molecules blocking phosphate anions. Therefore, the third-body effect, which has been studied at the half cell level, is expected to be utilized to enhance the cell performances of practical HT-PEMFC.

In summary, by alloying Pt metal with other metals and appropriately changing the carbon carrier, the problems related to Pt-based catalysts can be solved to a certain extent. In particular, the activity and durability of Pt-based catalysts in PA-doped HT-PEMFCs can be well maintained by carbon coating or heteroatom doping. In addition, the modification

of the catalyst layer structure may be an important and beneficial factor in reducing Pt loading on the cathode and enhancing resistance to PA poisoning.

## 2.2 Non-precious metal catalysts

Due to the scarcity and high price of Pt-group metals, as well as the poisoning effect of the phosphate anion of PA/PBI-based membranes on Pt-based catalysts in HT-PEMFC, low-cost, resource-rich and easy to prepare non-precious metal catalysts have received special attention in the past decades. Non-precious metal catalysts have been extensively studied in LT-PEMFC, such as transition metals (mainly Fe and/or Co) loaded on doped carbon (M-N/C), exhibiting comparable performance to Pt/C catalysts. Particularly, the Fe-N-C catalyst exhibits activity close to that of Pt in acidic electrolytes and exhibits encouraging performance in LT-PEMFC.<sup>5,58</sup> Wu *et al.* introduced iron containing species during aniline polymerization on the carbon black surface and then synthesized Fe and N co-doped Fe-N-C catalyst by high temperature pyrolysis under Ar + NH<sub>3</sub> atmosphere and

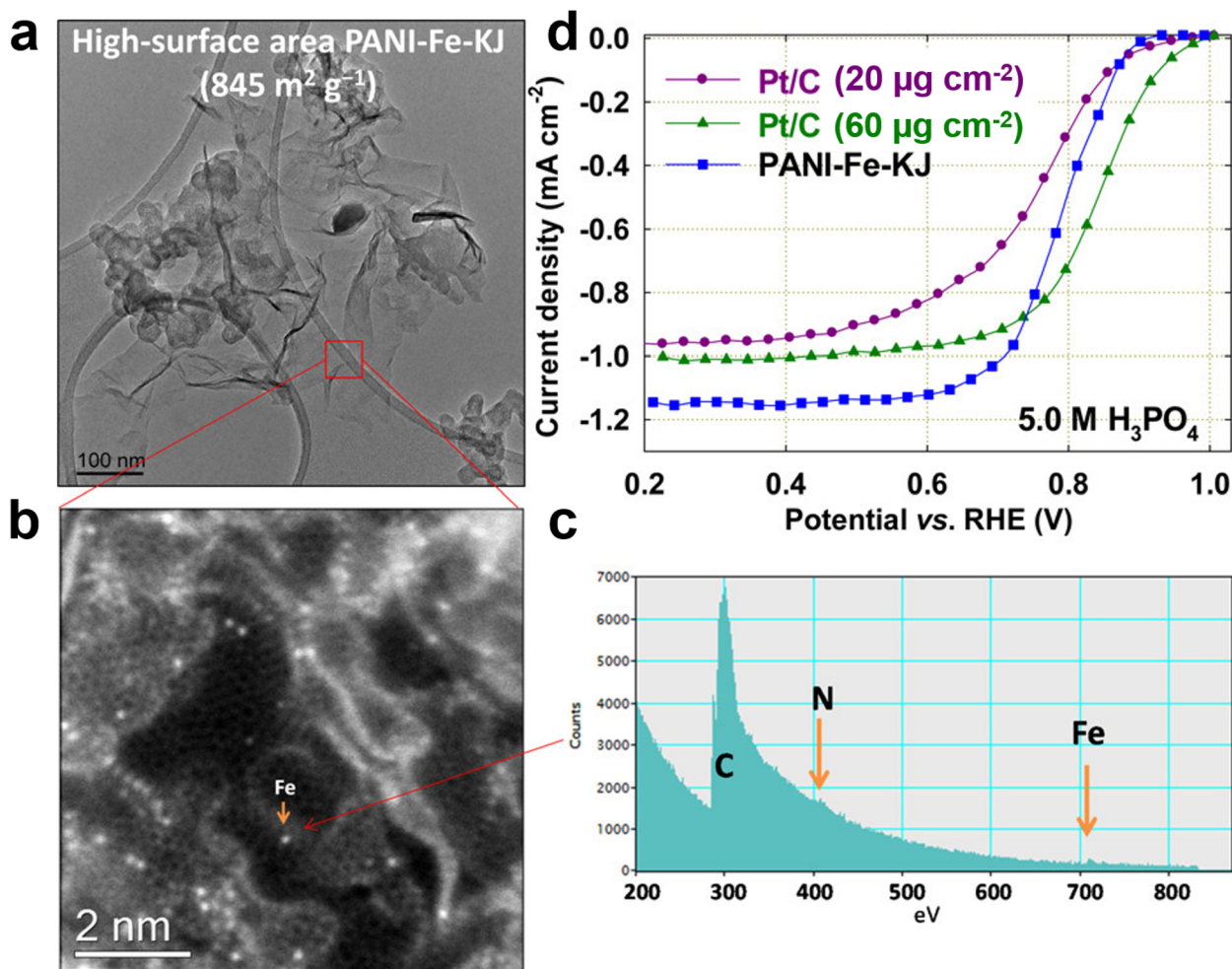


Fig. 11 (a) TEM image; (b) ADF-STEM of graphene sheet and (c) associated EEL spectra showing the presence of single Fe atoms on the surface of graphene; (d) comparison of ORR activity. Reprinted with permission from ref. 57. Copyright 2014, American Chemical Society.



acid leaching to the mixture of Fe species and polyaniline.<sup>59</sup> The as synthesized Fe–N–C catalyst exhibited good ORR catalytic activity and stability in acid electrolyte and fuel cell, but an inferior performance when compared to Pt catalyst. Moreover, the low density of active sites, insufficient stability, and poor three-phase interface within the cathode are still significant challenges faced by these M–N–C catalysts, and these issues are more prominent in HT-PEMFC. To the best of our knowledge, only a few reports have been published in this regard, and most of them include Fe-containing materials. Hu *et al.* affirmed the strong adsorption and poisoning effect of perchloric ions on ORR activity during the Fe–N–C based catalyst evaluation in dilute perchloric acid which is usually used in fuel cell catalyst development, but they found a negligible poisoning effect of phosphate anions when PA was used as the solution to evaluate the performance.<sup>60</sup> Accordingly, it was concluded that Fe–N–C could be used in HT-PEMFCs as a catalyst if a PA doped polybenzimidazole (PBI) membrane was employed. Zelenay *et al.*, using polyaniline (PANI), iron and carbon as raw materials, synthesized a catalyst (PANI–Fe–C) with a high surface area ( $845 \text{ m}^2 \text{ g}^{-1}$ ) by high-temperature method (Fig. 11a–c).<sup>57</sup> Electrochemical tests show that the prepared PANI–Fe–C catalyst can withstand high concentrations of phosphate ions and has better ORR performance than Pt/C catalyst at  $5.0 \text{ M H}_3\text{PO}_4$  (Fig. 11d). However, the performance achieved by this catalyst is still in low-temperature acidic electrolyte, and further research is needed to replace the Pt/C catalyst in PA doped HT-PEMFC. Atanassov *et al.* synthesized

iron–nitrogen–carbon (Fe–N–C) electrocatalysts using a sacrificial support method and discussed their performance for HT-PEMFC for the first time.<sup>61</sup>

Yu *et al.* for the first time prepared by simple pyrolysis highly microporous and mesoporous Fe–N–C catalysts, which are organometallic ethylenediamine tetraacetic acid (EDTA)–Fe complexes prepared from different mass ratios of iron salts and EDTA (Fig. 12a).<sup>62</sup> It is found that Fe exists mainly in the form of single atoms, and Fe particles also exist on the N-doped carbon support (Fig. 12b). The prepared single atom Fe catalyst was tested as an ORR electrocatalyst in HT-PEMFC, and the optimized catalyst had a peak power density of  $260 \text{ mW cm}^{-2}$  and a current density of  $1260 \text{ mA cm}^{-2}$  at  $0.2 \text{ V}$  (Fig. 12c). This high performance may be related to the high porosity, the presence of highly efficient active sites associated with monatomic Fe–N<sub>x</sub>, and the immunity of the iron–nitrogen catalyst to phosphate adsorption in the extremely harsh fuel cell operating environment. The synthesis of Fe single atoms, which usually involves the pyrolysis of inorganic iron salts, carbon and nitrogen precursors, has been extensively studied.<sup>63–65</sup> However, the loadings of Fe single atom catalysts reported to date are low, less than 2%, and, although considerable efforts have been invested to increase the loadings of Fe single atoms, the results are not satisfactory.<sup>66,67</sup> Improving the loading capacity of Fe single atoms is the ultimate goal of the practical application of non-precious metal catalysts in PEMFCs, and it is also one of the major challenges in this field. Cheng *et al.* prepared Fe single atoms loaded on highly conductive carbon



Fig. 12 (a) Schematic illustration of synthesis process for EDTA–Fe complex-based catalyst; (b) HAADF-STEM image of LEDFe<sub>5</sub>-NH<sub>3</sub>; (c) single-cell performance of HT-PEMFC at 1.5 bar O<sub>2</sub> pressure and 150 °C cell temperature. Reprinted with permission from ref. 62. Copyright 2014, American Chemical Society.





**Fig. 13** (a) Scheme for FeCu-N-CNTs synthesis; (b) AC-STEM; (c) polarization and power density curves of PA/PBI composite membrane cells using FeCu(1:0) and FeCu(4:1) cathodes at 160 and 230 °C. Reprinted with permission from ref. 69. Copyright 2021, Royal Society of Chemistry.

nanotubes (Fe SA) by simply annealing the carbon nitrogen precursor with hemin porcine (HP).<sup>68</sup> The Fe SA exhibits a  $E_{1/2}$  of 0.80 V, 27 mV more positive than that of Pt/C in 0.2 M  $\text{H}_3\text{PO}_4$  + 0.1 M  $\text{HClO}_4$  electrolyte due to its high phosphate resistance ability. The suitability of the synthesized Fe SA catalyst as a cathode was demonstrated in a HT-PEMFC using hydrogen as a fuel, with a peak power density of 266  $\text{mW cm}^{-2}$  and excellent stability at 240 °C. This method provides a simple and practical way for the development of highly efficient HT-PEMFC non-precious metal catalysts. Wang *et al.* developed a bimetallic FeCu electrocatalyst coordinated with atomically dispersed nitrogen doped carbon nanotubes (FeCu/N-CNTs) using a similar method (Fig. 13a and b).<sup>69</sup> The

peak power density of HT-PEMFC using FeCu/N-CNTs as the cathode at 230 °C is 302  $\text{mW cm}^{-2}$ , which is similar to that using Pt/C electrocatalyst (1  $\text{mg}_{\text{Pt}} \text{cm}^{-2}$ ) (Fig. 13c), but with much better stability. Compared with the phosphate poisoning caused by Pt/C, the PA activity of FeCu/N-CNTs is enhanced. DFT calculations indicate that the phosphate promoting effect is due to the stronger binding of phosphate at the Cu site, which reduces the activation energy barrier for  $\text{O}_2$  double bond cleavage and provides local protons, promoting the ORR of proton coupled electron transfer. Jiang *et al.* developed a high loading Fe single atom graphene catalyst (FeSA-G) using a one pot pyrolysis method (Fig. 14a and b).<sup>70</sup> The activity of the synthesized FeSA-G in



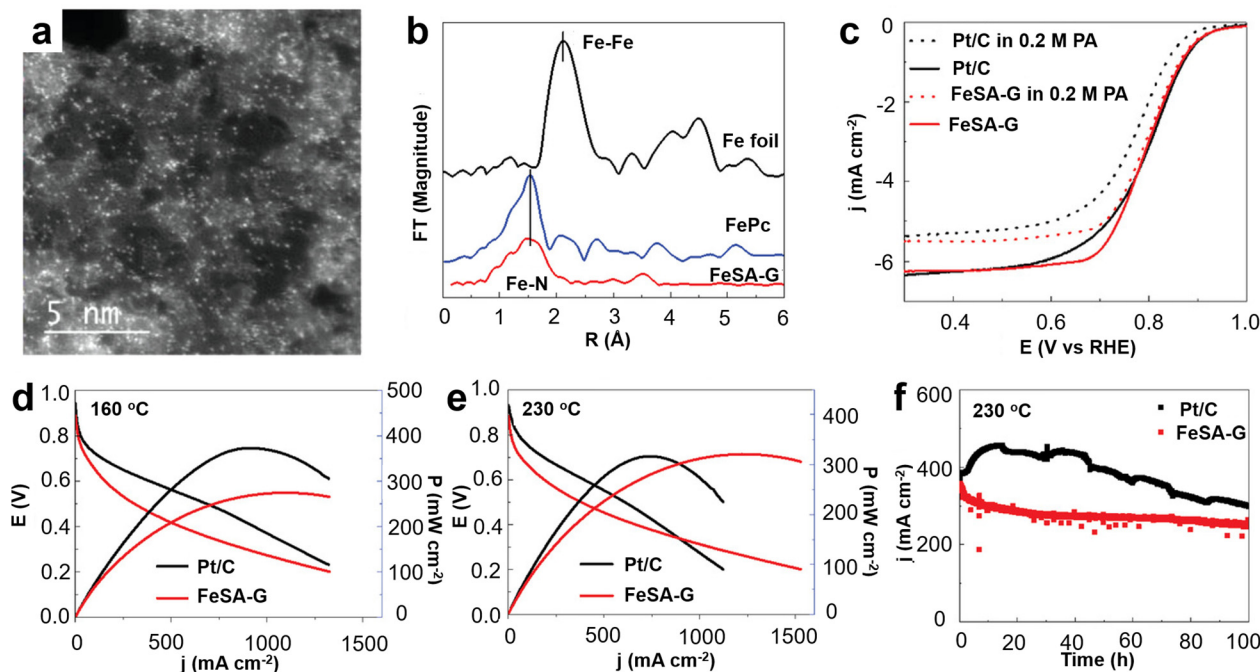


**Fig. 14** (a) AC-STEM images for FeSA-G; (b) Fourier transform of the EXAFS spectra of FeSA-G, FePc, and Fe foil; (c) linear scan voltammetry of FeSA-G and Pt/C; *J*-*V* and power density curves of high temperature PEMFCs at (d) 160 °C and (e) 230 °C; (f) stability of the cells at 0.5 V. Reprinted with permission from ref. 70. Copyright 2019, John Wiley & Sons.

the acidic electrolyte is similar to that of the Pt/C catalyst, but it has higher stability and greater phosphate anion tolerance (Fig. 14c). High temperature SiO<sub>2</sub> nanoparticle-doped phosphoric acid/polybenzimidazole (PA/PBI/SiO<sub>2</sub>) composite membrane cells utilizing a FeSA-G cathode with Fe SAC loading of 0.3 mg cm<sup>-2</sup> deliver a peak power density of 325 mW cm<sup>-2</sup> at 230 °C, better than the 313 mW cm<sup>-2</sup> obtained in the cell with a Pt/C cathode at a Pt loading of 1 mg cm<sup>-2</sup> (Fig. 14d and e). The cell with the FeSA-G cathode exhibits superior stability at 230 °C compared to the Pt/C cathode (Fig. 14f). The performance of this FeSA-G catalyst is one of the highest reported for non noble metal catalysts used as cathodes for HT-PEMFC to date. Fe-based catalysts are still the most widely studied transition metal catalyst for high temperature fuel cells. In addition, very few Co-based catalysts are used to improve the anti-phosphoric acid poisoning effect of HT-PEMFCs to obtain excellent catalytic performance. Eren *et al.* prepared a Co-N-C catalyst by surface modification of MWCNTs and confirmed the existence of a CoN/Co-N-C complex from the high-resolution analytical surface characterization. The results of the HT-PEMFCs single cell test show that the performances of CoN/MWCNT are superior to those of commercial Pt/C as cathode at 150 and 160 °C.<sup>71</sup>

The above results and discussion indicate that there is still much room for improvement in the development of non-precious metal ORR catalysts for HT-PEMFC. Therefore, a great deal of research work is required to develop high-performance non-precious metal catalysts with a view to replacing commercially available Pt-based catalysts.

### 3 High-temperature rotating disk electrode study of catalysts in phosphoric acid

Since the catalyst is evaluated directly in the MEA, the catalyst load, electrode structure, test conditions, PA distribution and other factors affect the cell performance.<sup>72,73</sup> In order to understand the inherent activity of catalysts, it is necessary to conduct half cell research.<sup>74</sup> The rotating disk electrode (RDE) system and electrochemistry work station can evaluate the ORR activity of different catalysts in liquid electrolyte. This method can avoid the uncertain factors during the fuel cell assembly and testing and provide the possibility for comparing different catalysts under the same conditions. The RDE method of dilute PA solution (1 mM–5 M) at room temperature (RT) is an effective strategy to study the effect of PA on catalyst activity.<sup>40,57</sup> However, the PA concentrations used in these studies were much lower than those in HT-PEMFC electrodes (~18 M, 95.5 wt%). Although phosphate adsorption strength was found to be comparable to sulfate adsorption on Pt(111),<sup>38</sup> the higher concentration and higher mobility of H<sub>3</sub>PO<sub>4</sub> than Nafion ionomer in the catalyst layer resulted in more significant suppression of reaction kinetics. What's more, HT-PEMFC may adsorb phosphate and oxygen differently at room temperature than at actual operating temperature. Some improved half-cell devices have been developed in the past,



including high temperature rotating disk electrodes,<sup>75</sup> pressurized rotating disk electrodes,<sup>76</sup> flow cells,<sup>77</sup> *etc.* By studying the ORR of Pt-based catalysts in PA, the basic principles of temperature effect, pressure effect, Tafel slope and transfer coefficient have been discussed. For example, in order to solve the problem that O<sub>2</sub> has low solubility and slow diffusion in hot concentrated phosphoric acid and the diffusion resistance can no longer be compensated by the Koutecky–Levich equation, Fleige *et al.* skilfully developed a pressurized RDE setup to increase the oxygen solubility and diffusion rate in electrolytes, which was an effective strategy but increased the complexity of the measurement and encountered the issue of unstable reference electrode potentials under a pressurized environment.<sup>78</sup> The fuel cell gas diffusion electrode is a porous structure with optimized pore size distribution and wetting characteristics. Using gas diffusion electrodes in electrochemical half-cells to characterize the activity of catalysts is attractive under conditions close to the actual operation of fuel cells. Zalitis *et al.* introduced a floating electrode design with a thin catalyst layer, whereby the catalyst activity was measured with efficient mass transport in 4.0 M HClO<sub>4</sub>.<sup>79</sup> Hu *et al.* designed and constructed a half cell device to measure the inherent activity of the catalyst for oxygen reduction reaction (ORR) under conditions close to those of the HT-PEMFC cathode (Fig. 15a and b).<sup>77</sup> By optimizing the hydrophobic characteristics of the electrode and the thickness of the catalyst layer, the catalytic activity of ORR catalysts can be quickly evaluated, and the ORR activity of typical Pt/C catalysts has been successfully measured in concentrated PA above 100 °C. The activity results obtained

through the half-cell setup are comparable to the RDE measurement results at room temperature and the fuel cell test results at high temperature (Fig. 15c), demonstrating the feasibility of this method in evaluating catalyst performance under HT-PEMFC conditions. However, these complex settings hinder the use of these methods in catalyst material research. Therefore, optimizing the detection structure to minimize the catalyst evaluation parameters for high-temperature RDE and MEA is imperative. Jia *et al.* used the HT-RDE device to study the ORR activity of Pt based catalysts (Fig. 15d and e).<sup>80</sup> Under conventional electrochemical schemes, it was observed that the reducing substance PA (H<sub>3</sub>PO<sub>3</sub>) undergoes oxidation by H<sub>3</sub>PO<sub>4</sub> reduction during cyclic voltammetry (CV) cycles. In order to obtain reliable ORR measurements, the testing plan was optimized to avoid the formation of H<sub>3</sub>PO<sub>3</sub>. Then, the author compared the ORR activity of a series of Pt based catalysts at room temperature using a rotating disc electrode (RT-RDE) under HClO<sub>4</sub>(aq.) and HClO<sub>4</sub> + H<sub>3</sub>-PO<sub>4</sub>(aq.) conditions. By analyzing the changes in oxygen adsorption peak area and ORR activity, the correlation between the catalyst's resistance to H<sub>3</sub>PO<sub>4</sub> anions and the changes in ORR activity was revealed. The enhanced ORR kinetics on alloy catalysts were also verified in MEA, with PtCo/C still more active than Pt/C. In addition, due to the high operating pressure of MEA and the low PA content in the catalyst layer, its activity is higher than that of HT-RDE. At the same testing temperature, the difference between HT-RDE and MEA is smaller than that between RT-RDE and MEA (Fig. 15f and g). Since the adsorption species and configuration of PA affect the binding energy, an in-depth

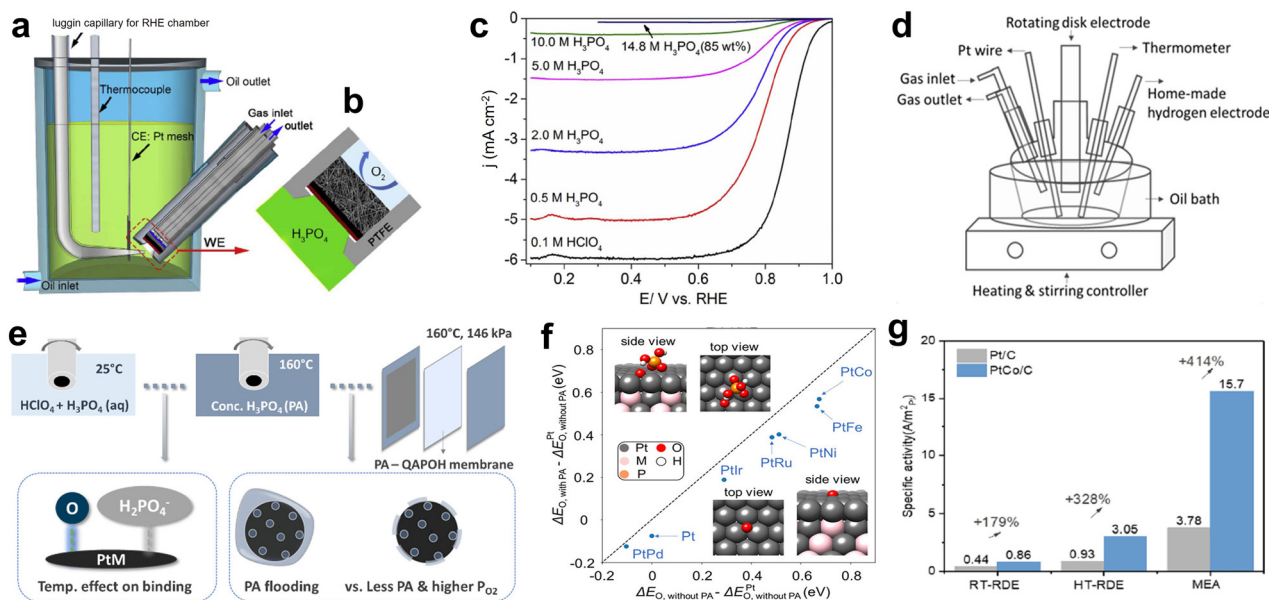


**Fig. 15** (a) The overall cross-sectional view and (b) the structure of the working electrode and the holder; (c) ORR polarization curves of 20 wt% Pt/C by RDE tests at room temperature in different electrolytes. Reprinted with permission from ref. 77. Copyright 2018, Elsevier. (d and e) Schematic of the HT-RDE setup; (f) DFT calculated O\* adsorption energy with/without phosphate (PA) on PtM(111)/Pt(111)skin; (g) comparison of the ORR specific activities of Pt/C and PtCo/C. Reprinted with permission from ref. 80. Copyright 2023, American Chemical Society.



**Table 1** Summary of previously reported catalysts and their application in HT-PEMFCs

Catalysts	Loading	Operating temperature	Condition	Peak power density (mW cm <sup>-2</sup> )	Durability	Year	Ref.
Pt-MoO <sub>x</sub> -MWCNT	0.25 mg <sub>Pt</sub> cm <sup>-2</sup>	140 °C	H <sub>2</sub> -O <sub>2</sub>	400	—	2010	81
sPt-OA	0.26 mg <sub>Pt</sub> cm <sup>-2</sup>	160 °C	H <sub>2</sub> /air	—	0.58 V@150 h	2015	32
Pt-Co alloy NPs	0.55 mg <sub>Pt</sub> cm <sup>-2</sup>	160 °C	H <sub>2</sub> -O <sub>2</sub>	640	—	2020	20
Pt-Co alloy NPs	0.55 mg <sub>Pt</sub> cm <sup>-2</sup>	160 °C	H <sub>2</sub> -air	290	0.6 V@84 h	2020	20
Pt/C	1 mg <sub>Pt</sub> cm <sup>-2</sup>	240 °C	H <sub>2</sub> -O <sub>2</sub>	325	0.6 V@12 h	2021	68
Cu-PtFe/NC	0.5 mg <sub>Pt</sub> cm <sup>-2</sup>	160 °C	H <sub>2</sub> -O <sub>2</sub>	793.5	0.7 V@100 h	2021	44
Cu-PtFe/NC	0.5 mg <sub>Pt</sub> cm <sup>-2</sup>	160 °C	H <sub>2</sub> -air	432.6	—	2021	44
CNT@SiO <sub>2</sub> -Pt	1 mg <sub>Pt</sub> cm <sup>-2</sup>	160 °C	H <sub>2</sub> -O <sub>2</sub>	765	0.7 V@100 h	2021	47
CNT@SiO <sub>2</sub> -Pt	1 mg <sub>Pt</sub> cm <sup>-2</sup>	160 °C	H <sub>2</sub> -air	486	—	2021	47
CNT@SiO <sub>2</sub> -Pt	1 mg <sub>Pt</sub> cm <sup>-2</sup>	220 °C	H <sub>2</sub> -O <sub>2</sub>	1061	—	2021	47
PtCo/C	0.91 mg <sub>Pt</sub> cm <sup>-2</sup>	160 °C	H <sub>2</sub> -O <sub>2</sub>	1350	—	2023	80
FeSA-G (high loading)	0.3 mg <sub>Fe</sub> cm <sup>-2</sup>	230 °C	H <sub>2</sub> -O <sub>2</sub>	325	0.6 V@100 h	2019	70
LEDFe5-NH <sub>3</sub>	3.8 mg <sub>Fe</sub> cm <sup>-2</sup>	150 °C	H <sub>2</sub> -O <sub>2</sub>	260	—	2020	62
FeSA/HP (high density)	0.6 mg <sub>Fe</sub> cm <sup>-2</sup>	240 °C	H <sub>2</sub> -O <sub>2</sub>	266	>0.6 V@100 h	2021	68
FeCu/N-CNTs	0.12 mg <sub>FeCu</sub> cm <sup>-2</sup>	230 °C	H <sub>2</sub> -O <sub>2</sub>	302	>0.5 V@100 h	2021	69

understanding from combining spectroscopic and simulation tools would be beneficial in future catalyst research.

The widespread use of RDE technology to rapidly characterize novel catalysts prepared from milligram quantities of material remains important for large-scale pre-selection of promising catalyst designs, but the catalyst must ultimately prove its performance and durability in MEA tests, which are very similar to real-world applications. However, the prediction of the results obtained by RDE on the performance of the environmental assessment system is often only applicable to the trend, not to the absolute value. In some cases, RDE-based assays systematically result in measuring artifacts rather than actual catalyst properties. The gap between these two technologies is a major barrier to quickly integrating promising electrocatalyst designs into actual PEM systems.

## 4 Summary and outlook

The commercialization and large-scale application of high-temperature proton exchange membrane fuel cells (HT-PEMFCs) require more durable and economical catalysts and exchange membranes. As shown in Table 1, among the cathode catalysts currently developed for HT-PEMFCs, atomically dispersed transition metal catalysts have become the most promising type of catalyst due to their abundant sources, high atom utilization, and performance comparable to noble metal-based catalysts. It is believed that as researchers gain a better understanding of the catalytic mechanism and synthesis concept of atomically dispersed catalysts, atomically dispersed transition metal carbon-based materials will most likely become commercial electrocatalysts in the future. Overall, the performance of catalysts can be improved through structural engineering, better dispersion of catalysts, and the development of corrosion-resistant carriers. However, the activity, durability and loading capacity of catalysts based on Pt group metals and non-precious metals remain challenging due to the stratification,

degradation, and poisoning of catalysts during long-term operation in high-temperature and PA environments. In addition, the large-scale development and application of catalysts for PA doped HT-PEMFCs still face the following problems that need to be urgently addressed:

1) The evolution and degradation mechanism in the catalytic layer of catalysts during long-term operation are still unclear. Although non precious metal catalysts have potential application prospects in LT-PEMFCs, their practicality in HT-PEMFCs still needs further research.

2) The proton conductivity of PA doped membranes strongly depends on the level of acid doping, and the loss of PA during operation hinders the stability of the cell.

3) HT PEMFCs have many influencing parameters and complex microenvironments which pose challenges to simulation experiments.

4) Lack of *in situ* characterization techniques to observe membrane and catalyst changes during operation. The redistribution of PA from the membrane to the catalyst layer is a key step that affects cell performance but is not fully understood by current characterization methods.

5) The HT-PEMFCs can be fed on the hydrogen produced from alcohol steam reforming reaction without further purification. This combination of heat reutilization can provide a new research field for the application and expansion of HT-PEMFCs and the use of green energy.

HT-PEMFCs have a high operating temperature and unique microenvironment which can expand the range of catalyst use. Some catalysts with poor activity or inability to be used at low temperatures may exhibit interesting phenomena in a HT-PEMFC system. During the operation of HT-PEMFC, the heat generated by the reaction can not only maintain the high temperature of the battery, but also serve as a heat source for some reactions, such as alcohol reforming reactions. Although there are many advantages to raising the temperature of PEMFCs to more than 100 °C, there are many challenges for both the catalyst and the entire system to fully understand the mechanism of PA-doped HT-PEMFCs. Combining theoretical simulation with advanced *in*



*situ* characterization techniques to design and manufacture efficient catalysts can effectively accelerate the commercialization process of HT-PEMFCs.

## Conflicts of interest

The authors declare no conflict of interest.

## Acknowledgements

This work was financially supported by the Key projects of National Natural Science Foundation of China (U22A20107), the key projects of the Henan Provincial Science and Technology R&D Program Joint Fund (222301420001), the Distinguished Young Scholars Innovation Team of Zhengzhou University (32320275), and Higher Education Teaching Reform Research and Practice Project of Henan Province (2021SJGLX093Y).

## References

- 1 B. C. H. Steele and A. Heinzl, Materials for fuel-cell technologies, *Nature*, 2001, **414**, 345–352.
- 2 L. Yan, P. Li, Q. Zhu, A. Kumar, K. Sun, S. Tian and X. Sun, Atomically precise electrocatalysts for oxygen reduction reaction, *Chem*, 2023, **9**, 280–342.
- 3 Y. Gu, Y. Liu and X. Cao, Evolving strategies for tumor immunotherapy: Enhancing the enhancer and suppressing the suppressor, *Natl. Sci. Rev.*, 2017, **4**, 161–163.
- 4 X. Tian, X. Zhao, Y.-Q. Su, L. Wang, H. Wang, D. Dang, B. Chi, H. Liu, E. J. M. Hensen, X. W. Lou and B. Y. Xia, Engineering bunched Pt-Ni alloy nanocages for efficient oxygen reduction in practical fuel cells, *Science*, 2019, **366**, 850–856.
- 5 X. X. Wang, M. T. Swihart and G. Wu, Achievements, challenges and perspectives on cathode catalysts in proton exchange membrane fuel cells for transportation, *Nat. Catal.*, 2019, **2**, 578–589.
- 6 M. Zhou, H.-L. Wang and S. Guo, Towards high-efficiency nanoelectrocatalysts for oxygen reduction through engineering advanced carbon nanomaterials, *Chem. Soc. Rev.*, 2016, **45**, 1273–1307.
- 7 D. Aili, D. Henkensmeier, S. Martin, B. Singh, Y. Hu, J. O. Jensen, L. N. Cleemann and Q. Li, Polybenzimidazole-based high-temperature polymer electrolyte membrane fuel cells: New insights and recent progress, *Electrochem. Energy Rev.*, 2020, **3**, 793–845.
- 8 E. Quartarone, S. Angioni and P. Mustarelli, Polymer and composite membranes for proton-conducting, high-temperature fuel cells: A critical review, *Materials*, 2017, **10**, 687.
- 9 R. K. Abdul Rasheed, Q. Liao, Z. Caizhi and S. H. Chan, A review on modelling of high temperature proton exchange membrane fuel cells (HT-PEMFCs), *Int. J. Hydrogen Energy*, 2017, **42**, 3142–3165.
- 10 S. Bose, T. Kuila, T. X. H. Nguyen, N. H. Kim, K.-t. Lau and J. H. Lee, Polymer membranes for high temperature proton exchange membrane fuel cell: Recent advances and challenges, *Prog. Polym. Sci.*, 2011, **36**, 813–843.
- 11 S.-F. Lu, S.-K. Peng and Y. Xiang, Perspectives on the research progress of bipolar interfacial polyelectrolyte membrane fuel cell, *Acta Phys.-Chim. Sin.*, 2016, **32**, 1859–1865.
- 12 Y. Oono, A. Sounai and M. Hori, Influence of the phosphoric acid-doping level in a polybenzimidazole membrane on the cell performance of high-temperature proton exchange membrane fuel cells, *J. Power Sources*, 2009, **189**, 943–949.
- 13 C. Wannek, I. Konradi, J. Mergel and W. Lehnert, Redistribution of phosphoric acid in membrane electrode assemblies for high-temperature polymer electrolyte fuel cells, *Int. J. Hydrogen Energy*, 2009, **34**, 9479–9485.
- 14 G.-B. Jung, C.-C. Tseng, C.-C. Yeh and C.-Y. Lin, Membrane electrode assemblies doped with H<sub>3</sub>PO<sub>4</sub> for high temperature proton exchange membrane fuel cells, *Int. J. Hydrogen Energy*, 2012, **37**, 13645–13651.
- 15 P. Boillat, J. Biesdorf, P. Oberholzer, A. Kaestner and T. J. Schmidt, Evaluation of neutron imaging for measuring phosphoric acid distribution in high temperature pemfc, *J. Electrochem. Soc.*, 2014, **161**, F192–F198.
- 16 S. Liu, M. Rasinski, Y. Rahim, S. Zhang, K. Wippermann, U. Reimer and W. Lehnert, Influence of operating conditions on the degradation mechanism in high-temperature polymer electrolyte fuel cells, *J. Power Sources*, 2019, **439**, 227090.
- 17 X. Xu, H. Wang, S. Lu, Z. Guo, S. Rao, R. Xiu and Y. Xiang, A novel phosphoric acid doped poly(ethersulphone)-poly(vinyl pyrrolidone) blend membrane for high-temperature proton exchange membrane fuel cells, *J. Power Sources*, 2015, **286**, 458–463.
- 18 F. Zhou, D. Singdeo and S. K. Kær, Investigation of the effect of humidity level of H<sub>2</sub> on cell performance of a HT-PEM fuel cell, *Fuel Cells*, 2019, **19**, 2–9.
- 19 Z. Zhang, Z. Xia, J. Huang, F. Jing, X. Zhang, H. Li, S. Wang and G. Sun, Uneven phosphoric acid interfaces with enhanced electrochemical performance for high-temperature polymer electrolyte fuel cells, *Sci. Adv.*, 2023, **9**, 1194.
- 20 S. Y. Lim, S. Martin, G. Gao, Y. Dou, S. B. Simonsen, J. O. Jensen, Q. Li, K. Norrman, S. Jing and W. Zhang, Self-standing nanofiber electrodes with Pt-Co derived from electrospun zeolitic imidazolate framework for high temperature pem fuel cells, *Adv. Funct. Mater.*, 2020, **31**, 2006771.
- 21 Y. Liu, W. Lehnert, H. Janßen, R. C. Samsun and D. Stolten, A review of high-temperature polymer electrolyte membrane fuel-cell (HT-PEMFC)-based auxiliary power units for diesel-powered road vehicles, *J. Power Sources*, 2016, **311**, 91–102.
- 22 X. Wang, Z. Li, Y. Qu, T. Yuan, W. Wang, Y. Wu and Y. Li, Review of metal catalysts for oxygen reduction reaction: From nanoscale engineering to atomic design, *Chem*, 2019, **5**, 1486–1511.
- 23 V. R. Stamenkovic, B. Fowler, B. S. Mun, G. Wang, P. N. Ross, C. A. Lucas and N. M. Marković, Improved oxygen reduction activity on pt<sub>3</sub>Ni(111) via increased surface site availability, *Science*, 2007, **315**, 493–497.



- 24 Y. Nie, L. Li and Z. Wei, Recent advancements in Pt and Pt-free catalysts for oxygen reduction reaction, *Chem. Soc. Rev.*, 2015, **44**, 2168–2201.
- 25 J. Greeley, I. E. Stephens, A. S. Bondarenko, T. P. Johansson, H. A. Hansen, T. F. Jaramillo, J. Rossmeisl, I. Chorkendorff and J. K. Nørskov, Alloys of platinum and early transition metals as oxygen reduction electrocatalysts, *Nat. Chem.*, 2009, **1**, 552–556.
- 26 J. K. Nørskov, J. Rossmeisl, A. Logadottir, L. Lindqvist, J. R. Kitchin, T. Bligaard and H. Jónsson, Origin of the overpotential for oxygen reduction at a fuel-cell cathode, *J. Phys. Chem. B*, 2004, **108**, 17886–17892.
- 27 S. Lu, X. Xu, J. Zhang, S. Peng, D. Liang, H. Wang and Y. Xiang, A self-anchored phosphotungstic acid hybrid proton exchange membrane achieved via one-step synthesis, *Adv. Energy Mater.*, 2014, **4**, 1400842.
- 28 V. R. Stamenkovic, B. S. Mun, M. Arenz, K. J. J. Mayrhofer, C. A. Lucas, G. Wang, P. N. Ross and N. M. Markovic, Trends in electrocatalysis on extended and nanoscale Pt-bimetallic alloy surfaces, *Nat. Mater.*, 2007, **6**, 241–247.
- 29 L. Bu, N. Zhang, S. Guo, X. Zhang, J. Li, J. Yao, T. Wu, G. Lu, J.-Y. Ma, D. Su and X. Huang, Biaxially strained PtPb/Pt core/shell nanoplate boosts oxygen reduction catalysis, *Science*, 2016, **354**, 1410–1414.
- 30 Y. Chen, S. Ji, C. Chen, Q. Peng, D. Wang and Y. Li, Single-atom catalysts: Synthetic strategies and electrochemical applications, *Joule*, 2018, **2**, 1242–1264.
- 31 M. Shao, Q. Chang, J. P. Dodelet and R. Chenitz, Recent advances in electrocatalysts for oxygen reduction reaction, *Chem. Rev.*, 2016, **116**, 3594–3657.
- 32 Y.-H. Chung, S. J. Kim, D. Y. Chung, H. Y. Park, Y.-E. Sung, S. J. Yoo and J. H. Jang, Third-body effects of native surfactants on Pt nanoparticle electrocatalysts in proton exchange fuel cells, *Chem. Commun.*, 2015, **51**, 2968–2971.
- 33 K. Miyabayashi, H. Nishihara and M. Miyake, Platinum nanoparticles modified with alkylamine derivatives as an active and stable catalyst for oxygen reduction reaction, *Langmuir*, 2014, **30**, 2936–2942.
- 34 J. Tao, X. Wang, M. Xu, C. Liu, J. Ge and W. Xing, Non-noble metals as activity sites for ORR catalysts in proton exchange membrane fuel cells (PEMFCs), *Ind. Chem. Mater.*, 2023, **1**, 388–409.
- 35 V. Stamenkovic, B. S. Mun, K. J. J. Mayrhofer, P. N. Ross, N. M. Markovic, J. Rossmeisl, J. Greeley and J. K. Nørskov, Changing the activity of electrocatalysts for oxygen reduction by tuning the surface electronic structure, *Angew. Chem., Int. Ed.*, 2006, **45**, 2897–2901.
- 36 X. Zhu, X. Tan, K. H. Wu, S. C. Haw, C. W. Pao, B. J. Su, J. Jiang, S. C. Smith, J. M. Chen, R. Amal and X. Lu, Intrinsic ORR activity enhancement of Pt atomic sites by engineering the d-band center via local coordination tuning, *Angew. Chem., Int. Ed.*, 2021, **60**, 21911–21917.
- 37 M. Weber, F. C. Nart, I. R. de Moraes and T. Iwasita, Adsorption of phosphate species on Pt(111) and Pt(100) as studied by in situ ftir spectroscopy, *J. Chem. Phys.*, 1996, **100**, 19933–19938.
- 38 R. Gisbert, G. García and M. T. M. Koper, Adsorption of phosphate species on poly-oriented pt and Pt(111) electrodes over a wide range of pH, *Electrochim. Acta*, 2010, **55**, 7961–7968.
- 39 A. Tanaka, R. Adzic and B. Nikolic, Oxygen reduction on single crystal platinum electrodes in phosphoric acid solutions, *J. Serb. Chem. Soc.*, 1999, **64**, 695–705.
- 40 Q. He, X. Yang, W. Chen, S. Mukerjee, B. Koel and S. Chen, Influence of phosphate anion adsorption on the kinetics of oxygen electroreduction on low index Pt(hkl) single crystals, *Phys. Chem. Chem. Phys.*, 2010, **12**, 12544–12555.
- 41 Q. He, B. Shyam, M. Nishijima, D. Ramaker and S. Mukerjee, Mitigating phosphate anion poisoning of cathodic Pt/C catalysts in phosphoric acid fuel cells, *J. Phys. Chem. C*, 2013, **117**, 4877–4887.
- 42 Z. Xia and S. Guo, Strain engineering of metal-based nanomaterials for energy electrocatalysis, *Chem. Soc. Rev.*, 2019, **48**, 3265–3278.
- 43 M. Luo and S. Guo, Strain-controlled electrocatalysis on multimetallic nanomaterials, *Nat. Rev. Mater.*, 2017, **2**, 17059.
- 44 W. Li, D. Wang, T. Liu, L. Tao, Y. Zhang, Y. C. Huang, S. Du, C. L. Dong, Z. Kong, Y. F. Li, S. Lu and S. Wang, Doping-modulated strain enhancing the phosphate tolerance on ptfе alloys for high-temperature proton exchange membrane fuel cells, *Adv. Funct. Mater.*, 2021, **32**, 2109244.
- 45 Y. Devrim, H. Devrim and I. Eroglu, Polybenzimidazole/SiO<sub>2</sub> hybrid membranes for high temperature proton exchange membrane fuel cells, *Int. J. Hydrogen Energy*, 2016, **41**, 10044–10052.
- 46 H. Wang, X. Li, X. Feng, Y. Liu, W. Kang, X. Xu, X. Zhuang and B. Cheng, Novel proton-conductive nanochannel membranes with modified SiO<sub>2</sub> nanospheres for direct methanol fuel cells, *J. Solid State Electrochem.*, 2018, **22**, 3475–3484.
- 47 G. Huang, Y. Li, S. Du, Y. Wu, R. Chen, J. Zhang, Y. Cheng, S. Lu, L. Tao and S. Wang, Silica-facilitated proton transfer for high-temperature proton-exchange membrane fuel cells, *Sci. China: Chem.*, 2021, **64**, 2203–2211.
- 48 S. S. Chougule, A. A. Jeffery, S. Roy Chowdhury, J. Min, Y. Kim, K. Ko, B. Sravani and N. Jung, Antipoisoning catalysts for the selective oxygen reduction reaction at the interface between metal nanoparticles and the electrolyte, *Carbon Energy*, 2023, **5**, e293.
- 49 H. Li, P. Wen, D. S. Itanze, Z. D. Hood, S. Adhikari, C. Lu, X. Ma, C. Dun, L. Jiang, D. L. Carroll, Y. Qiu and S. M. Geyer, Scalable neutral H<sub>2</sub>O<sub>2</sub> electrosynthesis by platinum diphosphide nanocrystals by regulating oxygen reduction reaction pathways, *Nat. Commun.*, 2020, **11**, 3928.
- 50 Z. Pu, J. Zhao, I. S. Amini, W. Li, M. Wang, D. He and S. Mu, A universal synthesis strategy for P-rich noble metal diphosphide-based electrocatalysts for the hydrogen evolution reaction, *Energy Environ. Sci.*, 2019, **12**, 952–957.
- 51 J. Kou, J. Zhu Chen, J. Gao, X. Zhang, J. Zhu, A. Ghosh, W. Liu, A. J. Kropf, D. Zemlyanov, R. Ma, X. Guo, A. K. Datye, G. Zhang, L. Guo and J. T. Miller, Structural and catalytic



- properties of isolated  $\text{Pt}^{2+}$  sites in platinum phosphide ( $\text{PtP}_2$ ), *ACS Catal.*, 2021, **11**, 13496–13509.
- 52 W. Tian, Y. Wang, W. Fu, J. Su, H. Zhang and Y. Wang,  $\text{PtP}_2$  nanoparticles on n,p doped carbon through a self-conversion process to core-shell Pt/ $\text{PtP}_2$  as an efficient and robust ORR catalyst, *J. Mater. Chem. A*, 2020, **8**, 20463–20473.
- 53 J.-H. Yu, K. P. Singh, S.-J. Kim, T.-H. Kang, K.-S. Lee, H. Kim, S. Ringe and J.-S. Yu, Active and stable  $\text{PtP}_2$ -based electrocatalysts solve the phosphate poisoning issue of high temperature fuel cells, *J. Mater. Chem. A*, 2023, **11**, 6413–6427.
- 54 Y. Li, L. Jiang, S. Wang and G. Sun, Influence of phosphoric anions on oxygen reduction reaction activity of platinum, and strategies to inhibit phosphoric anion adsorption, *Chin. J. Catal.*, 2016, **37**, 1134–1141.
- 55 D. Strmcnik, M. Escudero-Escribano, K. Kodama, V. R. Stamenkovic, A. Cuesta and N. M. Marković, Enhanced electrocatalysis of the oxygen reduction reaction based on patterning of platinum surfaces with cyanide, *Nat. Chem.*, 2010, **2**, 880–885.
- 56 Y.-H. Chung, D. Y. Chung, N. Jung and Y.-E. Sung, Tailoring the electronic structure of nanoelectrocatalysts induced by a surface-capping organic molecule for the oxygen reduction reaction, *J. Phys. Chem. Lett.*, 2013, **4**, 1304–1309.
- 57 Q. Li, G. Wu, D. A. Cullen, K. L. More, N. H. Mack, H. T. Chung and P. Zelenay, Phosphate-tolerant oxygen reduction catalysts, *ACS Catal.*, 2014, **4**, 3193–3200.
- 58 H. Yin, P. Yuan, B.-A. Lu, H. Xia, K. Guo, G. Yang, G. Qu, D. Xue, Y. Hu, J. Cheng, S. Mu and J.-N. Zhang, Phosphorus-driven electron delocalization on edge-type  $\text{FeN}_4$  active sites for oxygen reduction in acid medium, *ACS Catal.*, 2021, **11**, 12754–12762.
- 59 G. Wu, K. L. More, C. M. Johnston and P. Zelenay, High-performance electrocatalysts for oxygen reduction derived from polyaniline, iron, and cobalt, *Science*, 2011, **332**, 443–447.
- 60 Y. Hu, J. O. Jensen, C. Pan, L. N. Cleemann, I. Shypunov and Q. Li, Immunity of the Fe-N-C catalysts to electrolyte adsorption: Phosphate but not perchloric anions, *Appl. Catal., B*, 2018, **234**, 357–364.
- 61 R. Gokhale, T. Asset, G. Qian, A. Serov, K. Artyushkova, B. C. Benicewicz and P. Atanassov, Implementing pgm-free electrocatalysts in high-temperature polymer electrolyte membrane fuel cells, *Electrochem. Commun.*, 2018, **93**, 91–94.
- 62 F. Razmjooei, J.-H. Yu, H.-Y. Lee, B.-J. Lee, K. P. Singh, T.-H. Kang, H.-J. Kim and J.-S. Yu, Single-atom iron-based electrocatalysts for high-temperature polymer electrolyte membrane fuel cell: Organometallic precursor and pore texture tailoring, *ACS Appl. Energy Mater.*, 2020, **3**, 11164–11176.
- 63 A. Zitolo, V. Goellner, V. Armel, M.-T. Sougrati, T. Mineva, L. Stievano, E. Fonda and F. Jaouen, Identification of catalytic sites for oxygen reduction in iron- and nitrogen-doped graphene materials, *Nat. Mater.*, 2015, **14**, 937–942.
- 64 P. Chen, T. Zhou, L. Xing, K. Xu, Y. Tong, H. Xie, L. Zhang, W. Yan, W. Chu, C. Wu and Y. Xie, Atomically dispersed iron-nitrogen species as electrocatalysts for bifunctional oxygen evolution and reduction reactions, *Angew. Chem., Int. Ed.*, 2017, **56**, 610–614.
- 65 Y. J. Sa, D.-J. Seo, J. Woo, J. T. Lim, J. Y. Cheon, S. Y. Yang, J. M. Lee, D. Kang, T. J. Shin, H. S. Shin, H. Y. Jeong, C. S. Kim, M. G. Kim, T.-Y. Kim and S. H. Joo, A general approach to preferential formation of active Fe-N<sub>x</sub> sites in Fe-N/C electrocatalysts for efficient oxygen reduction reaction, *J. Am. Chem. Soc.*, 2016, **138**, 15046–15056.
- 66 Y. Chen, S. Ji, Y. Wang, J. Dong, W. Chen, Z. Li, R. Shen, L. Zheng, Z. Zhuang, D. Wang and Y. Li, Isolated single iron atoms anchored on N-doped porous carbon as an efficient electrocatalyst for the oxygen reduction reaction, *Angew. Chem., Int. Ed.*, 2017, **56**, 6937–6941.
- 67 L. Jiao, G. Wan, R. Zhang, H. Zhou, S. H. Yu and H. L. Jiang, From metal-organic frameworks to single-atom Fe implanted N-doped porous carbons: Efficient oxygen reduction in both alkaline and acidic media, *Angew. Chem., Int. Ed.*, 2018, **57**, 8525–8529.
- 68 Y. Cheng, J. Zhang, X. Wu, C. Tang, S.-Z. Yang, P. Su, L. Thomsen, F. Zhao, S. Lu, J. Liu and S. P. Jiang, A template-free method to synthesis high density iron single atoms anchored on carbon nanotubes for high temperature polymer electrolyte membrane fuel cells, *Nano Energy*, 2021, **80**, 105534.
- 69 Y. Cheng, M. Wang, S. Lu, C. Tang, X. Wu, J.-P. Veder, B. Johannessen, L. Thomsen, J. Zhang, S.-Z. Yang, S. Wang and S. P. Jiang, First demonstration of phosphate enhanced atomically dispersed bimetallic FeCu catalysts as Pt-free cathodes for high temperature phosphoric acid doped polybenzimidazole fuel cells, *Appl. Catal., B*, 2021, **284**, 119717.
- 70 Y. Cheng, S. He, S. Lu, J. P. Veder, B. Johannessen, L. Thomsen, M. Saunders, T. Becker, R. De Marco, Q. Li, S. Z. Yang and S. P. Jiang, Iron single atoms on graphene as nonprecious metal catalysts for high-temperature polymer electrolyte membrane fuel cells, *Adv. Sci.*, 2019, **6**, 1802066.
- 71 E. O. Eren, N. Özkan and Y. Devrim, Development of non-noble Co-N-C electrocatalyst for high-temperature proton exchange membrane fuel cells, *Int. J. Hydrogen Energy*, 2020, **45**, 33957–33967.
- 72 R. Haider, Y. Wen, Z.-F. Ma, D. P. Wilkinson, L. Zhang, X. Yuan, S. Song and J. Zhang, High temperature proton exchange membrane fuel cells: Progress in advanced materials and key technologies, *Chem. Soc. Rev.*, 2021, **50**, 1138–1187.
- 73 B. Hopfenmüller, R. Zorn, O. Holderer, O. Ivanova, W. Lehnert, W. Lüke, G. Ehlers, N. Jalarvo, G. J. Schneider, M. Monkenbusch and D. Richter, Fractal diffusion in high temperature polymer electrolyte fuel cell membranes, *J. Chem. Phys.*, 2018, **148**, 204906.
- 74 T. Lazaridis, B. M. Stühmeier, H. A. Gasteiger and H. A. El-Sayed, Capabilities and limitations of rotating disk electrodes versus membrane electrode assemblies in the investigation of electrocatalysts, *Nat. Catal.*, 2022, **5**, 363–373.



- 75 A. J. Appleby, Oxygen reduction on active platinum in 85% orthophosphoric acid, *J. Electrochem. Soc.*, 1970, **117**, 641–645.
- 76 S. J. Clouser, J. C. Huang and E. Yeager, Temperature dependence of the tafel slope for oxygen reduction on platinum in concentrated phosphoric acid, *J. Appl. Electrochem.*, 1993, **23**, 597–605.
- 77 Y. Hu, Y. Jiang, J. O. Jensen, L. N. Cleemann and Q. Li, Catalyst evaluation for oxygen reduction reaction in concentrated phosphoric acid at elevated temperatures, *J. Power Sources*, 2018, **375**, 77–81.
- 78 M. J. Fleige, G. K. H. Wiberg and M. Arenz, Rotating disk electrode system for elevated pressures and temperatures, *Rev. Sci. Instrum.*, 2015, **86**, 064101.
- 79 C. M. Zalitis, D. Kramer and A. R. Kucernak, Electrocatalytic performance of fuel cell reactions at low catalyst loading and high mass transport, *Phys. Chem. Chem. Phys.*, 2013, **15**, 4329–4340.
- 80 H. Lin, Z. Hu, K. H. Lim, S. Wang, L. Q. Zhou, L. Wang, G. Zhu, K. Okubo, C. Ling, Y. S. Kim and H. Jia, High-temperature rotating disk electrode study of platinum bimetallic catalysts in phosphoric acid, *ACS Catal.*, 2023, **13**, 5635–5642.
- 81 R. Vellacheri, S. M. Unni, S. Nahire, U. K. Kharul and S. Kurungot, Pt-MOO<sub>x</sub>-carbon nanotube redox couple based electrocatalyst as a potential partner with polybenzimidazole membrane for high temperature polymer electrolyte membrane fuel cell applications, *Electrochim. Acta*, 2010, **55**, 2878–2887.

